Eco-Engineering of Seawalls—An Opportunity for Enhanced Climate Resilience From Increased Topographic Complexity

Md Salauddin[1,2]*, John J. O'Sullivan[1,2], Soroush Abolfathi[3] and Jonathan M. Pearson[3]

[1] UCD Dooge Centre for Water Resources Research, School of Civil Engineering, University College Dublin, Dublin, Ireland,
[2] UCD Earth Institute, University College Dublin, Dublin, Ireland, [3] School of Engineering, University of Warwick, Coventry, United Kingdom

In the context of "green" approaches to coastal engineering, the term "eco-engineering" has emerged in recent years to describe the incorporation of ecological concepts (including artificially water-filled depressions and surface textured tiles on seawalls and drilled holes in sea structures) into the conventional design process for marine infrastructures. Limited studies have evaluated the potential increase in wave energy dissipation resulting from the increased hydraulic roughness of ecologically modified sea defences which could reduce wave overtopping and consequent coastal flood risks, while increasing biodiversity. This paper presents results of small-scale laboratory investigations of wave overtopping on artificially roughened seawalls. Impulsive and non-impulsive wave conditions with two deep-water wave steepness values (=0.015 and 0.06) are evaluated to simulate both swell and storm conditions in a two-dimensional wave flume with an impermeable 1:20 foreshore slope. Measurements from a plain vertical seawall are taken as the reference case. The seawall was subsequently modified to include 10 further test configurations where hydraulic effects, reflective of "eco-engineering" interventions, were simulated by progressively increasing seawall roughness with surface protrusions across three length scales and three surface densities. Measurements at the plain vertical seawall compared favorably to empirical predictions from the EurOtop II Design Manual and served as a validation of the experimental approach. Results from physical model experiments showed that increasing the length and/or density of surface protrusions reduced overtopping on seawalls. Benchmarking of test results from experiments with modified seawalls to reference conditions showed that the mean overtopping rate was reduced by up to 100% (test case where protrusion density and length were maximum) under impulsive wave conditions. Results of this study highlight the potential for eco-engineering interventions on seawalls to mitigate extreme wave overtopping hazards by dissipating additional wave energy through increased surface roughness on the structure.

Keywords: climate change, coastal resilience, eco-engineering, ecologically enhanced seawall, vertical breakwaters, wave overtopping, coastal flooding

INTRODUCTION

As our climate continues to change, coastal defences will be subjected to increasing pressures from rising sea levels and a higher frequency of storm surges from extreme climatic events. Damage to sea defences and significant flooding of coastal areas from wave overtopping will present risks to lives and properties and this will need to be managed (IPCC, 2014, 2018; Vitousek et al., 2017). Approaches for managing flood risks in coastal zones have traditionally relied on "hard" engineered sea defence solutions which are costly to both install and maintain, and can be visually unattractive. The longer-term sustainability of such approaches is coming under increased scrutiny because of adverse economic, environmental and ecological impacts. More specifically, the negative impacts of "hard" engineered solutions include losses of biodiversity in adjacent coastal zones (Barbier et al., 2011; Browne and Chapman, 2014) and the lack of dynamic response to climate change (Borsje et al., 2011; Temmerman et al., 2013; Pontee et al., 2016; Vuik et al., 2016; Morris et al., 2018). Eco-retrofitting of engineered infrastructures can contribute to climate adaptation by integrating natural systems into existing structures and incorporating building integrated living systems (BILS), as advocated by Birkeland (2003, 2009), can produce positive ecological benefits.

In recent years, the term "eco-engineering" or "hard eco-engineering" has been spotlighted in many studies (Dafforn et al., 2015; Perkol-Finkel and Sella, 2015; Strain et al., 2018a,b; Evans et al., 2019; Salauddin et al., 2020a; O'Sullivan et al., 2020; O'Shaughnessy et al., 2020; Evans et al., 2021) to describe the adoption of biomimicry-based engineered interventions in sea defence structures that enhance biodiversity and species richness on the surface of the infrastructures and in surrounding areas. Recent research has focused on the introduction to existing coastal infrastructures of artificial, water-filled features to enhance the ecological well-being of these structures. A common element of these features, regardless of whether they are "additive" (as in the case of bolt-on rock pools (Morris et al., 2017; Naylor et al., 2017, 2018; Strain et al., 2017; Hall et al., 2019; **Figures 1A,B**), or "textured concrete" or "textured surface" tiles (Perkol-Finkel and Sella, 2015; Naylor et al., 2017; MacArthur et al., 2018; **Figure 1C**) on sea defences) or "subtractive" (as in the case of "drill-cored rock pools" in intertidal breakwaters (Browne and Chapman, 2014; Firth et al., 2014a,b; Evans et al., 2016; Hall et al., 2018; Waltham and Sheaves, 2020; **Figure 1D**), is that they serve to increase the topographic complexity and the surface roughness of the structures to which they are added.

To date, research efforts have focused on investigating the ecological benefits of such interventions and this is well reported in scientific literature (see for example, Barbier et al., 2011; Borsje et al., 2011; Temmerman et al., 2013; Browne and Chapman, 2014; Evans et al., 2016, 2019; Morris et al., 2018; Strain et al., 2018a,b). To the authors' knowledge however, there have been no studies that investigated the potential benefits of these ecological interventions in the context of reducing wave overtopping and flood risk as a result of the increased wave damping that accrues from the additional surface roughness of modified sea defences. Consequently, there remains a research gap in assessing the hydraulic performance of coastal defences that have been artificially roughened by ecological interventions such as "vertipools" (Hall et al., 2018, 2019) or "flowerpots" (Browne and Chapman, 2011; Strain et al., 2018a,b). Overtopping of waves on sea defences in this regard, refers to the situation where wave run-up levels of the largest waves are greater than the crest height of the structure, resulting in a volume of water flowing over the structure (such as a seawall, a dike, or a breakwater). Overtopping of waves can cause damage to the structure itself but may also present significant flood hazards in areas behind the structure with risks of harm to both people and property. More hazardous conditions can result in situations of extreme events. This paper presents laboratory-based physical modelling investigations on the wave overtopping characteristics on artificially roughened seawalls. The seawalls were not tested with scaled models of the actual biomimicry-based interventions of the type shown in **Figure 1**, but rather, included a range of generic roughnesses configurations of varying scale and density using circular elements that allowed for an assessment of overtopping for various roughness of sea defence structure. The experimental set-up in this study is adapted from the well-established small-scale wave flume investigation guidance of Wolters et al. (2009) and EurOtop (2018). Both wave and overtopping characteristics at a plain vertical seawall (reference case), as well as at artificially roughened seawalls, were assessed and experimental results relating to overtopping were compared to empirical predictions using the established EurOtop (2018) guidance. It was anticipated that the increased topographic complexity from increasing the surface roughness of the tested seawalls may mitigate wave overtopping (reduction in volumes) on the sea structure by reducing wave height and wave energy, and this was largely proven to be the case. The findings of this paper will be of interest to both researchers and practitioners engaged in designing new and retrofitting existing sea defences, particularly where enhancing biodiversity and climate resilience of the defence infrastructures is important.

EMPIRICAL PREDICTIONS OF WAVE OVERTOPPING

Wave overtopping is a key process at the wave-structure interface of sea defences and is often expressed as the mean overtopping discharge (q in m^3/s per m) per linear meter width of structure. Considerable field and laboratory-based research efforts have focused on developing and improving reliable prediction methods for estimating mean overtopping discharges at sea defences (Franco et al., 1994; Van der Meer and Janssen, 1994; Besley, 1998; TAW, 2002; Allsop et al., 2005; Victor et al., 2012; Salauddin et al., 2017; Salauddin and Pearson, 2019a, 2020; Dong et al., 2020a,b). However, it was not until 2007 that the first design guidance for estimating overtopping at sea defences was published by EurOtop (Pullen et al., 2007). This EurOtop manual has recently been superseded by a second EurOtop (2018) guidance manual, which reflects the addition of more recently acquired

FIGURE 1 | Examples of eco-engineering interventions—**(A)** artificial water-filled depressions (credit: Ecostructure), **(B)** "flowerpots" used for enhancing sustainability in Sydney Harbour (credit: R. Morris), **(C)** textured concrete tiles attached to the seawall (credit: Ecostructure), **(D)** "drill-cored rock pools" in intertidal breakwaters (credit: Ecostructure).

data and an improved understanding of the complex wave-structure interactions and resulting overtopping processes. Recent laboratory investigations on plain vertical seawalls by Dong et al. (2018) and Salauddin and Pearson (2018, 2019a) showed that the empirical prediction formulae in EurOtop (2018) approximated closely the overtopping measurements for both impulsive and non-impulsive wave conditions.

The existing tools for predicting overtopping at vertical seawalls are mainly based on incident wave characteristics at the wave-structure interface for impulsive and non-impulsive wave conditions. Non-impulsive or pulsating wave conditions are those associated with deeper waters where wave heights are small relative to depths. Non-impulsive waves do not break at the structure interface, whereas impulsive wave conditions occur in situations where waves break on the coastal defence structure. Under impulsive conditions, wave induced forces can be very significant, ranging from 10 to 40 times those observed for non-impulsive wave conditions (Oumeraci, 1994; Allsop et al., 1996; Bruce et al., 2010).

EurOtop (2018) proposes empirical relationships for classification of wave conditions at vertical walls. Eq. 1 and 2 present the criteria for non-impulsive and impulsive wave conditions, respectively:

$$\frac{h_t^2}{(H_{m0}L_{m-1,0})} > 0.23 \tag{1}$$

$$\frac{h_t^2}{(H_{m0}L_{m-1,0})} \leq 0.23 \tag{2}$$

where, H_{m0} is the significant wave height calculated from spectral analysis, h_t is the water depth at the toe of the structure, $L_{m-1,0}$ is the deep-water wavelength based on spectral wave period ($= \frac{gT_{m-1,0}^2}{2\pi}$) and $T_{m-1,0}$ denotes the spectral wave period derived from spectral analysis of incident waves.

Mean overtopping rates at vertical walls with foreshore slopes are estimated by Eq. 3 for non-impulsive conditions, and Eqs. 4 and 5 are used for impulsive conditions:

$$\frac{q}{\sqrt{gH_{m0}^3}} = 0.05exp\left(-2.78\frac{R_c}{H_{m0}}\right) \tag{3}$$

$$\frac{q}{\sqrt{gH_{m0}^3}} = 0.011 \left(\frac{H_{mo}}{h_t s_{m-1,0}}\right)^{0.5} exp\left(-2.2\frac{R_c}{H_{m0}}\right)$$

$$for \ 0 < \frac{R_c}{H_{m0}} < 1.35 \qquad (4)$$

$$\frac{q}{\sqrt{gH_{m0}^3}} = 0.0014 \left(\frac{H_{mo}}{h_t s_{m-1,0}}\right)^{0.5} for \ \frac{R_c}{H_{m0}} \geq 1.35 \quad (5)$$

where, R_c denotes the crest freeboard of the structure, g is the gravitational acceleration and $s_{m-1,0}$ defines the wave steepness $\left(= \frac{H_{m0}}{L_{m-1,0}}\right)$.

To identify the hazards associated with extreme wave overtopping events, it has become increasingly common to consider the maximum individual wave overtopping volume (V_{max}) in an overtopping sequence in combination with the mean overtopping rate. Besley (1998) studied wave overtopping at plain vertical seawalls and proposed Eq. 6 for predicting V_{max} [Eq.6 is also recommended in EurOtop (2018)]:

$$V_{max} = a(ln \ N_{ow})^{1/b} \qquad (6)$$

where, V_{max} is the peak wave overtopping volume per linear meter width of structure, N_{ow} defines the number of overtopping waves and a and b denote the Weibull scale and shape factors, respectively. The Weibull scale factor for impulsive and non-impulsive wave conditions is:

$$a = \left(\frac{1}{\Gamma\left(1+\frac{1}{b}\right)}\right)\left(\frac{qT_m}{P_{ov}}\right) \qquad (7)$$

where, Γ denotes the gamma function and P_{ov} indicates the proportion of overtopping waves.

Weibull shape parameters for inclusion in Eq. 6 are determined from Eqs. 8 and 9, for non-impulsive and impulsive wave conditions, respectively (Besley, 1998):

$$b = \begin{cases} 0.66 & for \quad s_{m-1,0} = 0.02 \\ 0.88 & for \quad s_{m-1,0} = 0.04 \end{cases} \qquad (8)$$

$$b = 0.85 \qquad (9)$$

EurOtop (2018) recommends the use of Eqs. 10 and 11 for estimating the proportion of overtopping waves, P_{ov}, for non-impulsive and impulsive wave attacks, respectively, at vertical walls:

$$P_{ov} = \frac{N_{ow}}{N_w} = exp\left[-1.21\left(\frac{R_c}{H_{m0}}\right)^2\right] \qquad (10)$$

$$P_{ov} = \frac{N_{ow}}{N_w} = \left[\frac{h_t^2}{(H_{m0}L_{m-1,0})}\left(\frac{R_c}{H_{m0}}\right)\right]^{-1} \text{ with a minimum predicted by Eq. 10} \qquad (11)$$

where N_w indicates the number of waves in a test sequence.

It is generally expected that the wave-by-wave overtopping volumes in an overtopping sequence follow a two-parameter Weibull distribution (Pearson et al., 2002; EurOtop, 2018), as described in Eq. 12:

$$P_v = 1 - exp\left[-\left(\frac{V}{a}\right)^b\right] \qquad (12)$$

where, V is the overtopping volume per wave [m³ per m], P_v is the probability that an individual overtopping volume will not exceed V, and a and b denote the scale and shape factors of the Weibull distribution function (Eqs. 7–9).

METHODOLOGY

Experimental Set-Up and Test Conditions

The laboratory investigations presented in this paper were undertaken in a two-dimensional wave channel, with a working section 22 m long, 0.6 m wide and 1 m high (**Figure 2**), located at the Water Research Facility, in University of Warwick, United Kingdom. The wave channel was equipped with a piston type wavemaker with an active wave absorption system, capable of generating both regular and random wave sequences. An impermeable sloping foreshore with a uniform slope of 1:20 was constructed in front of a vertical seawall. The plain (smooth) vertical seawall (0.25 m high) was made of thick PVC board and positioned vertically across the entire width of the flume. Following reference tests of the plain seawall, the seawall was modified by including 10 no. different test combinations which included initially an array of drilled holes (5 mm), which were subsequently fitted with surface protrusions of varying length (0.01, 0.03, and 0.05 m) and surface density (25 stems/0.01 m², 50 stems/0.01 m², and 98 stems/0.01 m²). Protrusions were arranged in a regular rectangular pattern, and simulated a range of increased roughnesses on the seawall to reflect the more complex topography that may typically be associated with the retrofitting of biomimicry-based engineered interventions in marine infrastructures. The surface protrusions comprised semi-rigid plastic elements, 5 mm in diameter, which were sealed to the vertical seawall. Images of experiments are included in **Figure 2**. For all experiments, incident wave characteristics (height and period) and wave overtopping characteristics (mean overtopping discharge, proportion of overtopping waves and individual overtopping volumes) were measured. The experimental behaviour of the plain seawall served as the reference condition to which results from the other experimental configurations were compared. This experimental philosophy, which increased progressively in complexity as the length and density of surface roughness elements increased, allowed the effects of the changes in surface topography to be directly observed.

Six wire resistance wave gauges were positioned along the wave channel to measure the incident wave conditions (height and period) in this study. Each wave gauge worked independently with an independent channel containing two parallel metal probes that related the resistance across the probes to water surface elevation. Wave condition measurements were conducted following the 3-point methodology of Mansard and Funke (1980)
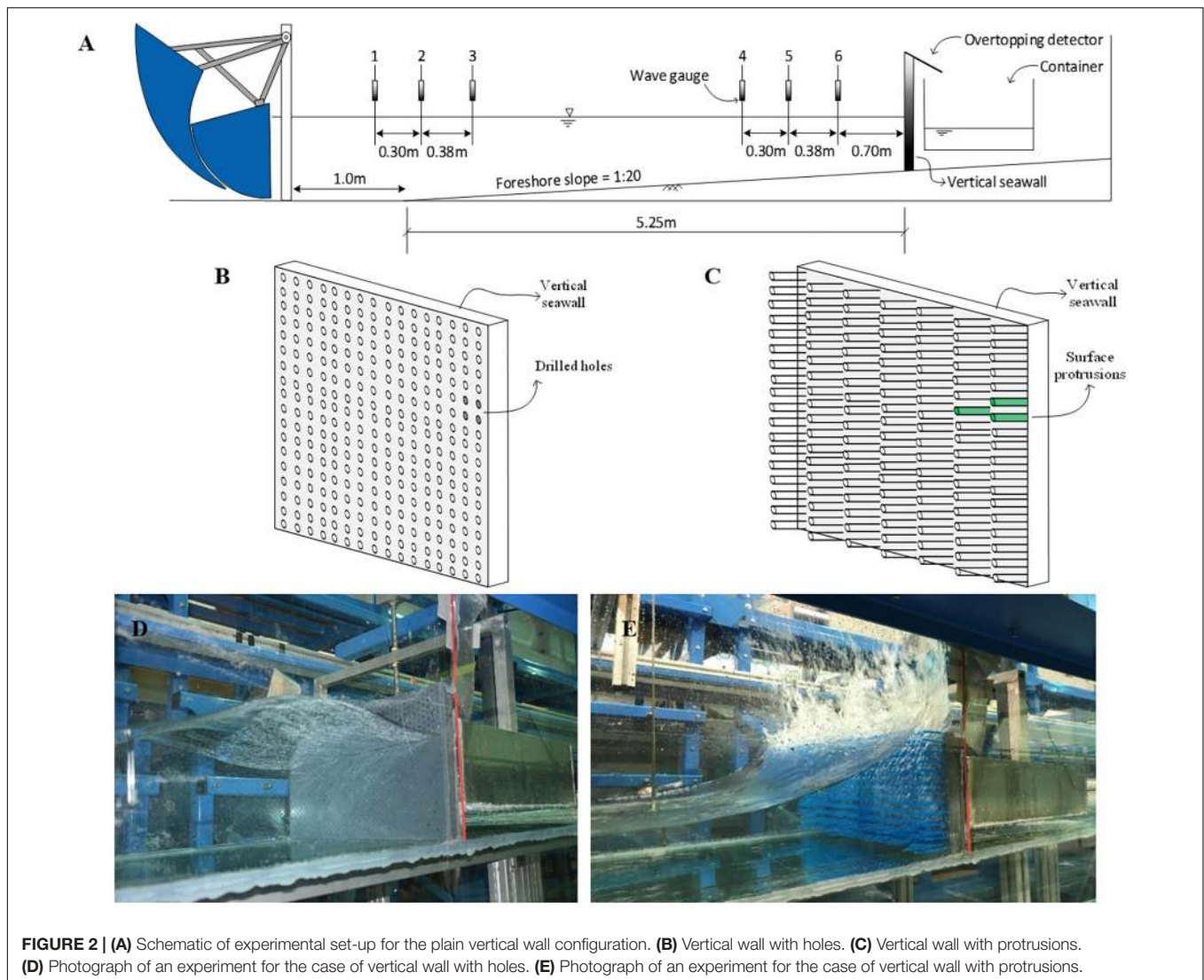
FIGURE 2 | (A) Schematic of experimental set-up for the plain vertical wall configuration. **(B)** Vertical wall with holes. **(C)** Vertical wall with protrusions.
(D) Photograph of an experiment for the case of vertical wall with holes. **(E)** Photograph of an experiment for the case of vertical wall with protrusions.

that recommends the use of three wave gauges to separate the incident and reflected waves. Accordingly, wave condition was recorded at two locations in the flume with one group of three wave gauges (WG 1–3 in **Figure 2**) being located near the wave paddle to measure the water surface elevations at relatively deep water, and a second set of three wave gauges (WG 4–6 in **Figure 2**) being placed in the nearshore region close to the structure to determine the shallow water wave conditions (near the seawall). The water surface elevations were recorded using a WG8USB wave gauge controller (Edinburgh Design Ltd.), capable of recording data from 8 channels. Water surface elevation data were then further processed to obtain calculated wave heights and wave periods (see sample data in **Supplementary Figure 1**). A reflection analysis using the least squares method enabled the separation of reflected waves from incident waves. To reduce possible uncertainties in determining incident and reflected inshore wave conditions, all the experiments for inshore conditions in the test matrix were repeated without the structure being in place.

Overtopping discharges were directed via a chute into a collection tank suspended from a loadcell. Individual wave overtopping events were identified by installing an overtopping detector with two metal strips along the crest of the structure serving as a switch which was closed by the overtopping water. Wave-by-wave overtopping volumes in a test sequence were calculated by measuring the increment in mass of water in the measuring container after each overtopping event, following the method described by Pearson et al. (2001); Bruce et al. (2009) and Salauddin and Pearson (2019a). A syphon mechanism was designed and installed to allow continuous measurement of overtopping for the test cases with a higher range of overtopping discharges.

All experiments were conducted for (the period of) approximately 1,000 random waves generated with a standard JONSWAP spectrum $\gamma = 3.3$. Both non-impulsive and impulsive wave attacks were studied with two deep-water wave steepness values of 0.015 and 0.06 (**Table 1**), representing swell and storm conditions, respectively. The incident wave heights varied from

TABLE 1 | T_p [s] values for tested combinations of s_{0p} and H_{m0} [m] in this study.

H_{m0}	0.05	0.06	0.07	0.08	0.09	0.1	0.12	0.14	0.16
s_{0p}									
0.015	1.46	1.60	1.73	1.85	1.96	2.07	2.26	2.44	2.61
0.06	0.73	0.80	0.86	0.92	0.98	1.03	1.13	1.22	1.31

0.05 to 0.16 m at the toe of the vertical wall for each nominal wave steepness. Two water depths of 0.09 and 0.16 m (toe) were tested in this study. Geometrical scaling of 1 in 50 was applied to the design test wave conditions. A matrix of 12 wave conditions was therefore undertaken for each experimental configuration, resulting in a total of 132 tests across the 11 configurations (1A to 5C in **Table 2**). The experiments included measurements to parameterise average overtopping rates and to determine the proportion of overtopping waves in addition to maximum individual overtopping volumes. Details of all tests and wave conditions are included in **Table 2**.

Approaches for minimising scale and model effects were considered throughout the experimental programme. The laboratory set-up for the experiments in this study adopted the well-established guidelines for small-scale two-dimensional wave flume investigations in EurOtop (2018) and HYDRALAB III (Wolters et al., 2009). Following Wolters et al. (2009), scale effects were minimised by ensuring that significant inshore wave heights were not less than 30 mm (tested wave heights in this study ranged from 50 to 150 mm, see **Table 2**). As also recommended by Wolters et al. (2009) and EurOtop (2018),

each test was conducted with a sequence of no less than 1,000 pseudo-random waves, representing a typical storm duration of 3-h, where both swell and storm wave conditions were included. Model effects in tests from the reflection of the model boundaries were minimised by an active wave absorption system in the flume. The efficacy of this system in minimising model effects from boundary reflections was confirmed in preliminary experimental tests where no seawall was present ("bare" flume). Results of these tests, in comparison to seawall tests, showed good agreement between wave heights across the full range of tested wave conditions.

System Accuracy

Prior to carrying out experiments, the accuracy of the overtopping measurement method was inspected using the techniques reported in Pearson et al. (2001) and Salauddin and Pearson (2019a). To replicate a known sequence of wave overtopping events, known volumes of water were added to the overtopping measuring tank passing through the crest of the structure. The data from the loadcell and overtopping detector were then analysed using a specifically developed algorithm to identify the individual overtopping volumes in the test sequence.

The true overtopping volume (pre-measured) for each event was subsequently compared to measured values from the calibration experiments (as shown in **Supplementary Table 1**) to verify the accuracy of the measurement system. Results indicate that the measured total overtopping volume differed only marginally (0.62%) from the actual (given) volumes, confirmed by a root mean square error (RMSE) of 9.98 ml. However,

TABLE 2 | Overview of test conditions.

| Experimental configuration	Test series	Toe water depth, h_t [m]	Relative freeboard, R_c/H_{m0} [–]	Nominal wave steepness, s_{0p} [–]	Significant wave height, H_{m0} [m]
Plain vertical seawall	1A	0.09 and 0.16	0.5–4.5	0.015 0.060	0.05–0.15
Vertical seawall with drilled holes	2A	0.09 and 0.16	0.5–4.5	0.015 0.060	0.05–0.15
Seawall with protrusions of 0.01 m in length (98 stems/100 mm^2)	3A	0.09 and 0.16	0.5–4.5	0.015 0.060	0.05–0.15
Seawall with protrusions of 0.01 m in length (50 stems/100 mm^2)	3B	0.09 and 0.16	0.5–4.5	0.015 0.060	0.05–0.15
Seawall with protrusions of 0.01 m in length (25 stems/100 mm^2)	3C	0.09 and 0.16	0.5–4.5	0.015 0.060	0.05–0.15
Seawall with protrusions of 0.03 m in length (98 stems/100 mm^2)	4A	0.09 and 0.16	0.5–4.5	0.015 0.060	0.05–0.15
Seawall with protrusions of 0.03 m in length (50 stems/mm^2)	4B	0.09 and 0.16	0.5–4.5	0.015 0.060	0.05–0.15
Seawall with protrusions of 0.03 m in length (25 stems/100 mm^2)	4C	0.09 and 0.16	0.5–4.5	0.015 0.060	0.05–0.15
Seawall with protrusions of 0.05 m in length (98 stems/100 mm^2)	5A	0.09 and 0.16	0.5–4.5	0.015 0.060	0.05–0.15
Seawall with protrusions of 0.05 m in length (50 stems/100 mm^2)	5B	0.09 and 0.16	0.5–4.5	0.015 0.060	0.05–0.15
Seawall with protrusions of 0.05 m in length (25 stems/100 mm^2)	5C	0.09 and 0.16	0.5–4.5	0.015 0.060	0.05–0.15

for the relatively small overtopping events, a larger deviation between measured and actual overtopping volumes was observed (**Supplementary Table 1**). The larger deviations are likely to be associated with a reduced sensitivity in the load cell for measuring these smaller volumes which are in the range of 5–9 ml.

## Validation of Reference Condition

The measurements for the case of the plain vertical seawall were taken as the benchmark or reference condition and the test data for the roughened wall configurations were compared to this reference case to evaluate the performance of the modified seawalls. Mean overtopping rates, the proportion of overtopping waves and the maximum individual overtopping volumes were determined for each experimental configuration and then compared with the predictions of EurOtop (2018). The data presented in **Figure 3** indicates good agreement between measured and predicted overtopping discharges for the case of non-impulsive test conditions. The dimensionless mean overtopping rates for impulsive wave conditions are compared with EurOtop (2018) empirical predictions (Eq. 5) in **Figure 4**. Good agreement between measured data and empirical predictions is observed.

The measured probability of overtopping waves for the benchmark experiments are compared with the predicted values of EurOtop (2018) for both impulsive and non-impulsive wave conditions in **Supplementary Figure 2**. The results for the tested conditions in this study correlate reasonably well with the empirical predictions of EurOtop (2018), increasing
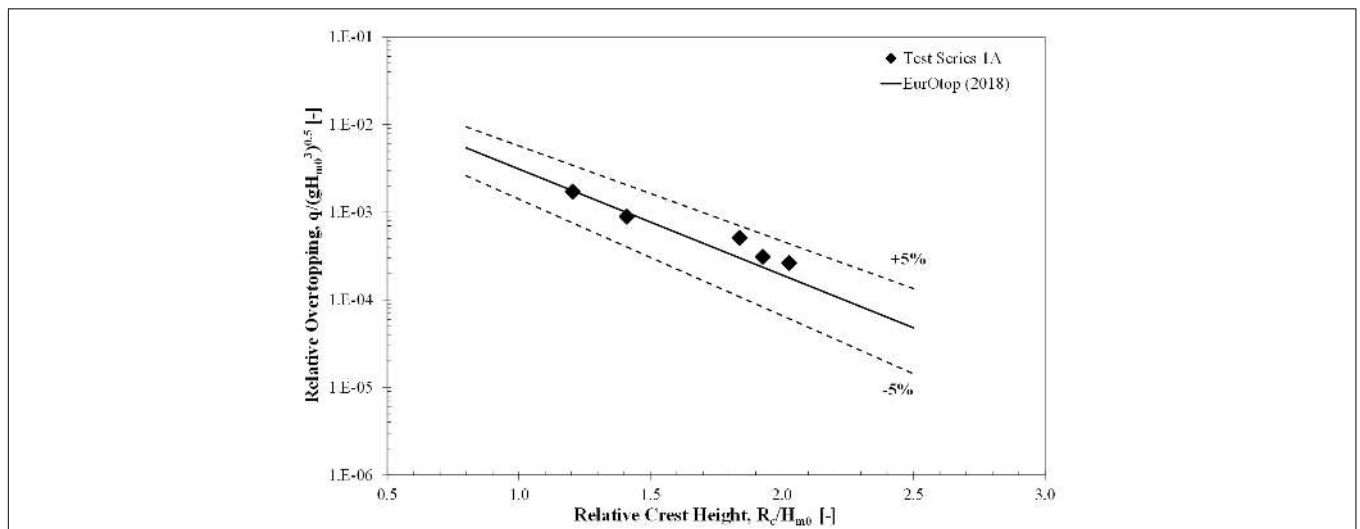
FIGURE 3 | Wave overtopping discharge on a plain vertical seawall (reference case), subjected to non-impulsive wave conditions (solid line represents predicted values of EurOtop, 2018, with 90% confidence interval).
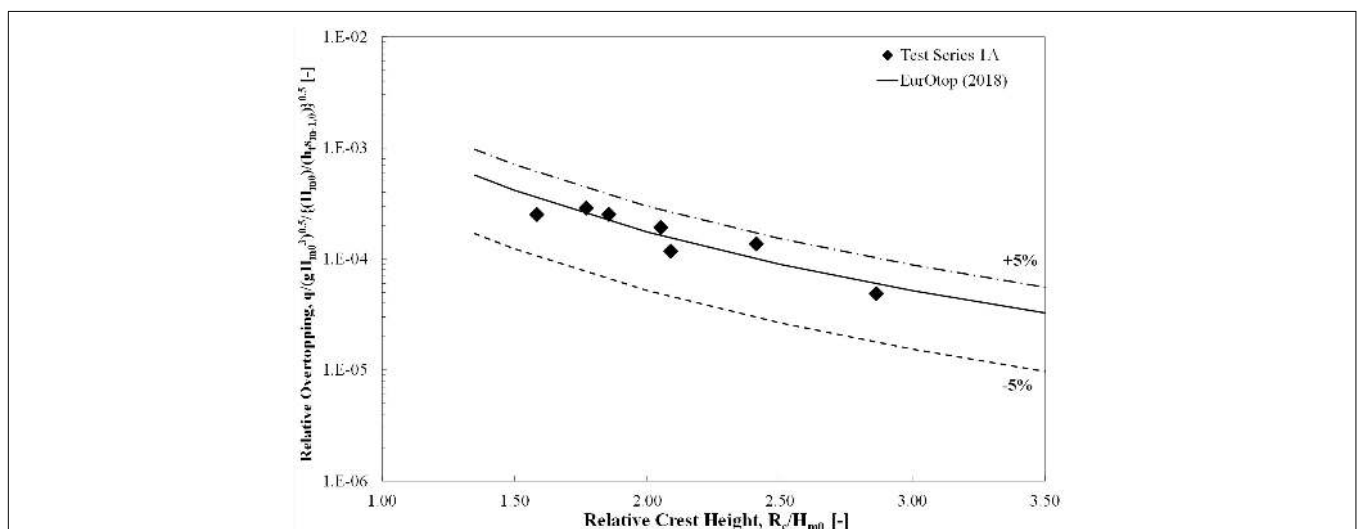
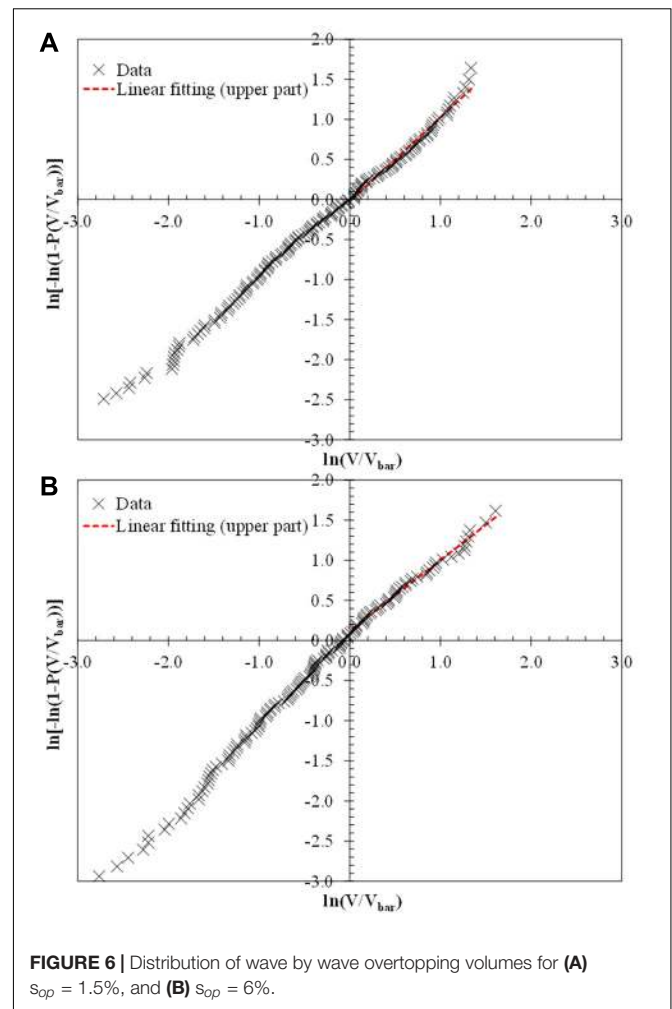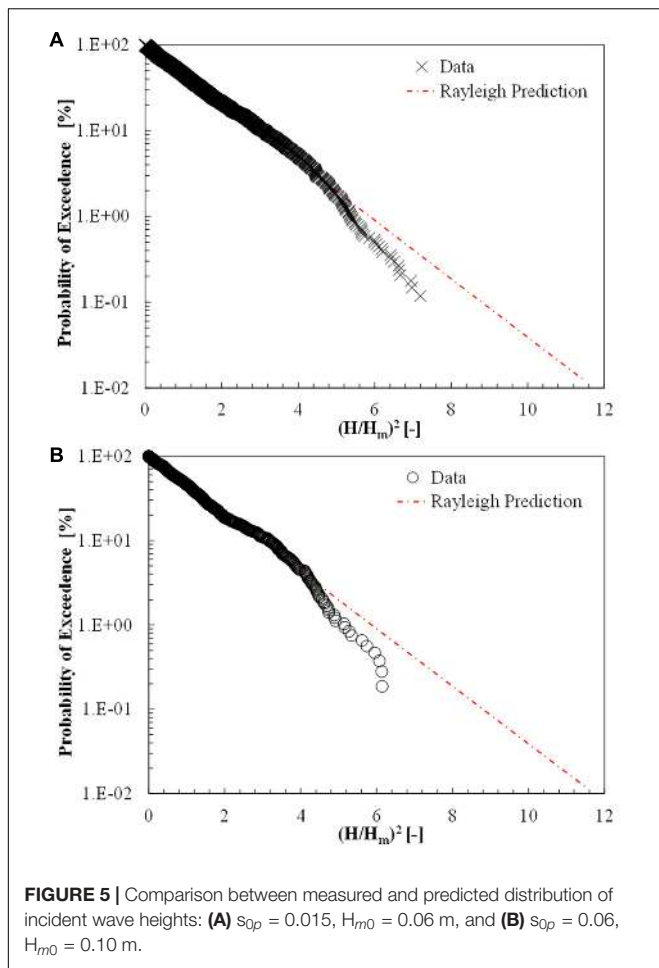

FIGURE 4 | Wave overtopping discharge on a plain vertical seawall (reference case), subjected to impulsive wave conditions (solid line represents predicted values of EurOtop, 2018, with 90% confidence interval).

FIGURE 5 | Comparison between measured and predicted distribution of incident wave heights: **(A)** s_{0p} = 0.015, H_{m0} = 0.06 m, and **(B)** s_{0p} = 0.06, H_{m0} = 0.10 m.

FIGURE 6 | Distribution of wave by wave overtopping volumes for **(A)** s_{op} = 1.5%, and **(B)** s_{op} = 6%.

confidence in the robustness of the EurOtop prediction method for estimating P_{ov} at plain vertical walls.

Furthermore, the maximum individual wave overtopping volumes in an overtopping test sequence for the reference case (plain vertical wall) are compared with the prediction of EurOtop (2018) in **Supplementary Figure 3** under both non-impulsive and impulsive wave attacks. The results show that measurements for the reference case compare favourably with EurOtop predictions.

It is therefore evident from the comparison between the measured overtopping characteristics and EurOtop predictions that the overtopping measurements of the reference configuration (i.e., plain vertical seawall) are in good agreement with the predictions.

RESULTS

Incident Wave Heights

In general, the incident wave heights in relatively deep waters follow the Rayleigh distribution whereas in nearshore regions, the distribution of incident wave heights deviates from the Rayleigh distribution (Battjes and Groenendijk, 2000; Goda, 2009; EurOtop, 2018; Dong et al., 2020b). The Rayleigh
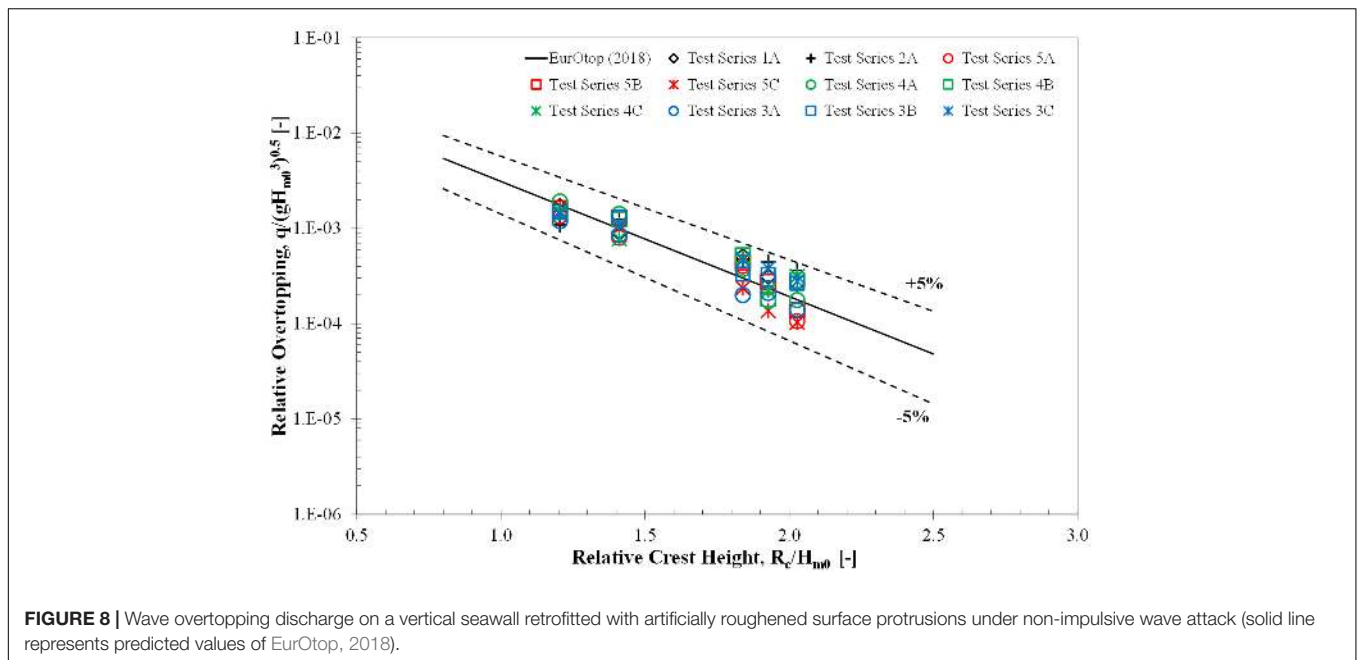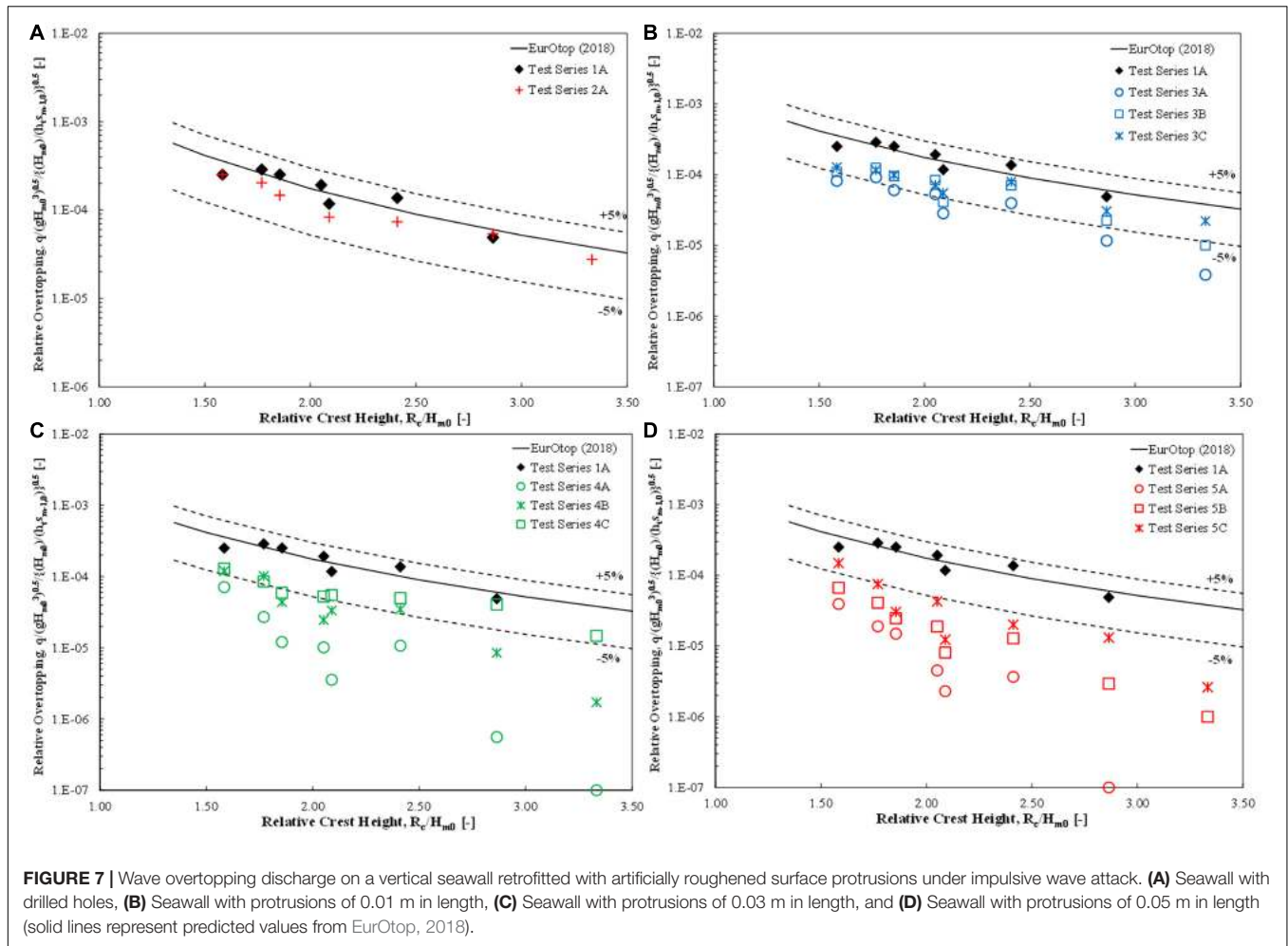
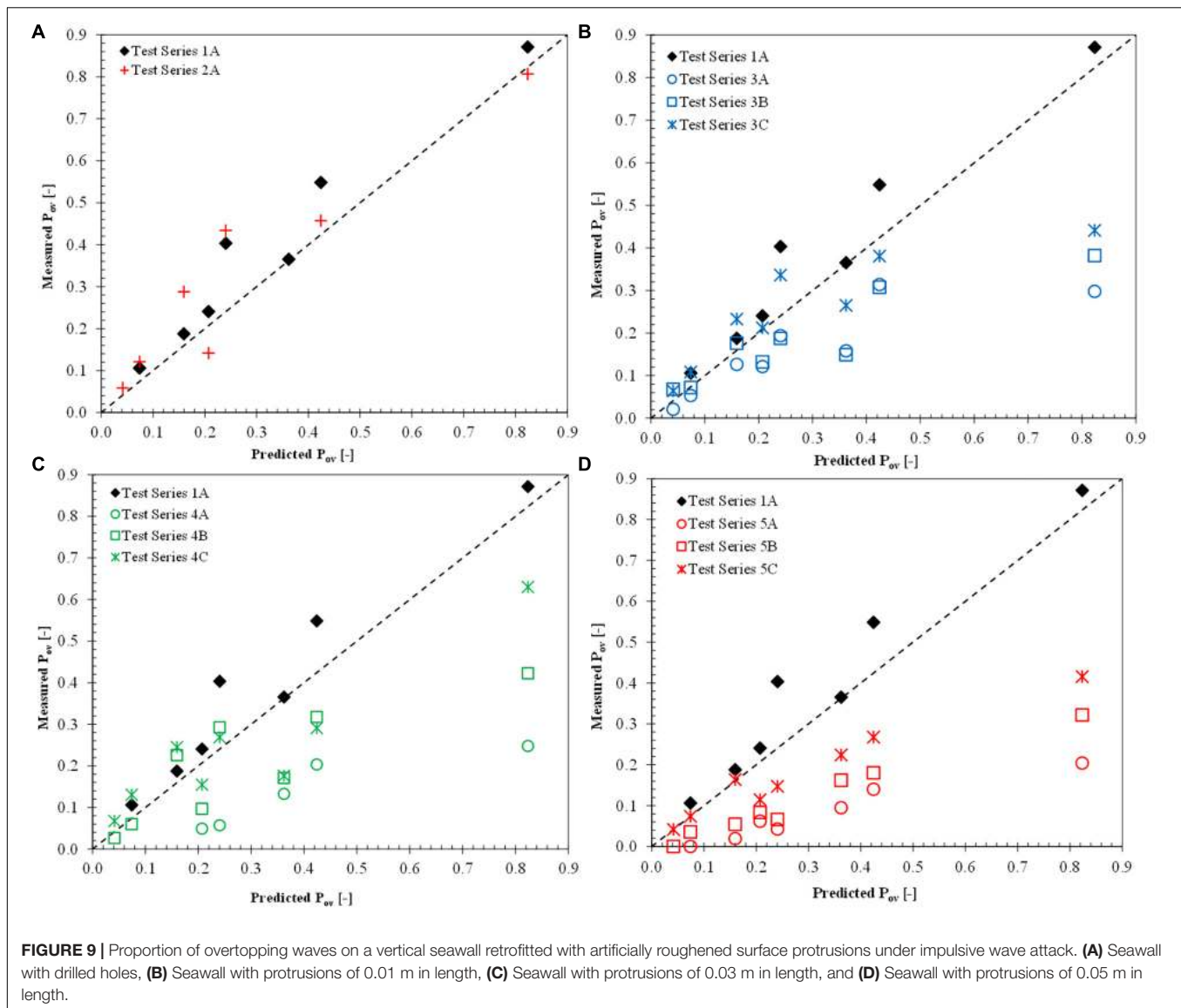distribution of wave heights can be expressed as:

$$F_H = 1 - exp\left[-\left(\frac{H}{H_{rms}}\right)^2\right] \qquad (13)$$

where, H denotes the individual wave height and H_{rms} represents the root mean square of the wave height.

For the two wave conditions tested in this study, the distribution of incident wave heights is compared to the predicted Rayleigh distribution in **Figure 5**. The individual wave heights (H) in **Figure 5** are normalised with mean square wave height (H_m). The measured data is shown to correlate well with the Rayleigh distribution for all but the extreme (largest) waves in the test sequence. Deviations from the theoretical distribution for extreme waves were not unexpected and have been previously observed in similar experimental programmes (e.g., Abolfathi et al., 2018; Dong et al., 2018, 2020b; Salauddin and Pearson, 2019a,b). Such deviations are typically associated with the breaking of waves close to the wave paddle under depth-limited wave conditions.

FIGURE 7 | Wave overtopping discharge on a vertical seawall retrofitted with artificially roughened surface protrusions under impulsive wave attack. **(A)** Seawall with drilled holes, **(B)** Seawall with protrusions of 0.01 m in length, **(C)** Seawall with protrusions of 0.03 m in length, and **(D)** Seawall with protrusions of 0.05 m in length (solid lines represent predicted values from EurOtop, 2018).

FIGURE 8 | Wave overtopping discharge on a vertical seawall retrofitted with artificially roughened surface protrusions under non-impulsive wave attack (solid line represents predicted values of EurOtop, 2018).

FIGURE 9 | Proportion of overtopping waves on a vertical seawall retrofitted with artificially roughened surface protrusions under impulsive wave attack. **(A)** Seawall with drilled holes, **(B)** Seawall with protrusions of 0.01 m in length, **(C)** Seawall with protrusions of 0.03 m in length, and **(D)** Seawall with protrusions of 0.05 m in length.

Distribution of Individual Overtopping Volumes

Measured individual overtopping volumes for the two tested conditions are shown in **Figure 6** on a Weibull scale, where V is the wave-by-wave overtopping volume, $P(V)$ is the probability that the volume of an individual overtopping event will equal or exceed a volume V and V_{bar} represents the mean overtopping volume. The linearity of the data in **Figure 6** confirms that the measured individual overtopping volumes follow the two-parameter Weibull distribution in accordance with the existing well-established literature.

For the prediction of maximum overtopping volumes in an overtopping sequence, the shape parameter, b, of the Weibull distribution (Eq. 4) is determined from the gradient of the linear regression line of the distribution. Larger overtopping volumes are typically of most concern in terms of the climate resilience of coastal infrastructures. Hence, the common approach (see for

example, Pearson et al., 2002; Zanuttigh et al., 2013; Salauddin et al., 2020b) for determining the Weibull shape parameter for the tested conditions by fitting to the higher proportion of individual overtopping volumes (where $V > V_{bar}$) in the extreme tail of the Weibull plot, was adopted (**Figure 6**).

Mean Overtopping Rates
Artificially Roughened Conditions

The non-dimensional mean overtopping discharges for the tested retrofit cases with respect to the relative freeboard of the structure are presented in **Figure 7** for impulsive wave conditions. **Figure 7** also compares the mean overtopping measurements from these test cases with the empirical predictions from EurOtop (2018). The uncertainty in the predictions derived from EurOtop (2018) is represented by including 5% upper and lower limits to the predictions. The overall trend of data corresponding to Test Series 2A (drilled holes) is similar to that from the
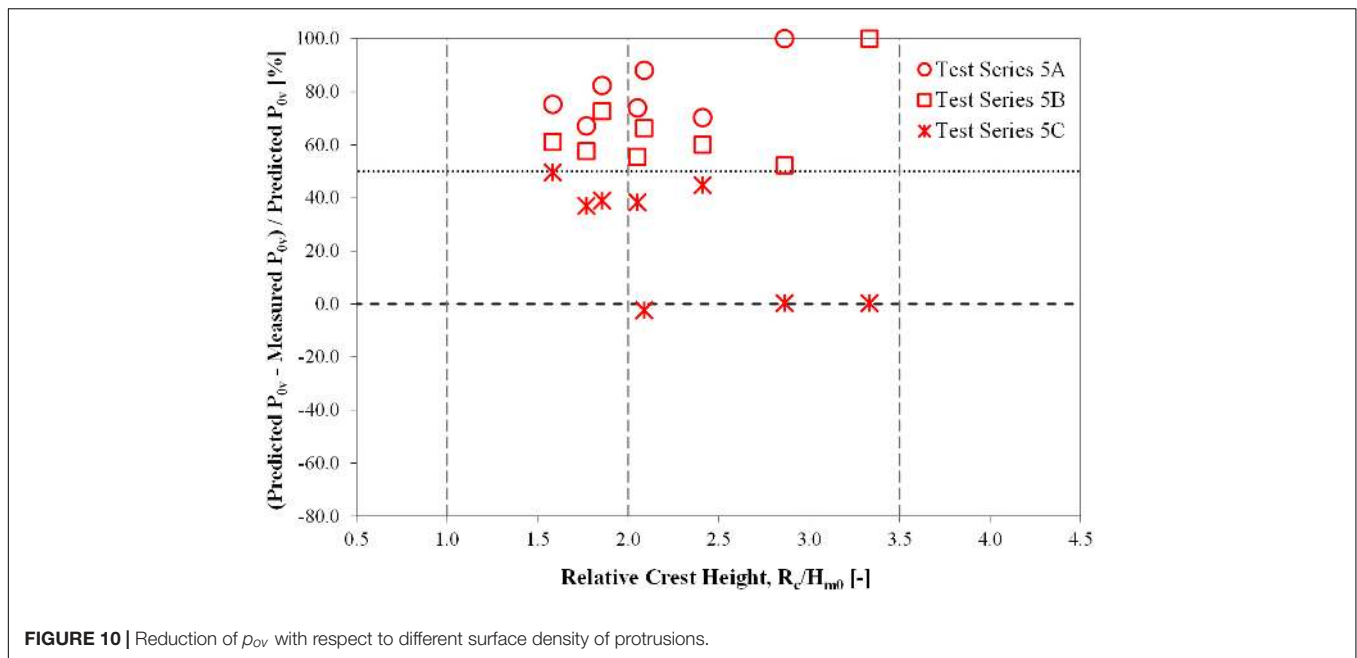
FIGURE 10 | Reduction of p_{ov} with respect to different surface density of protrusions.
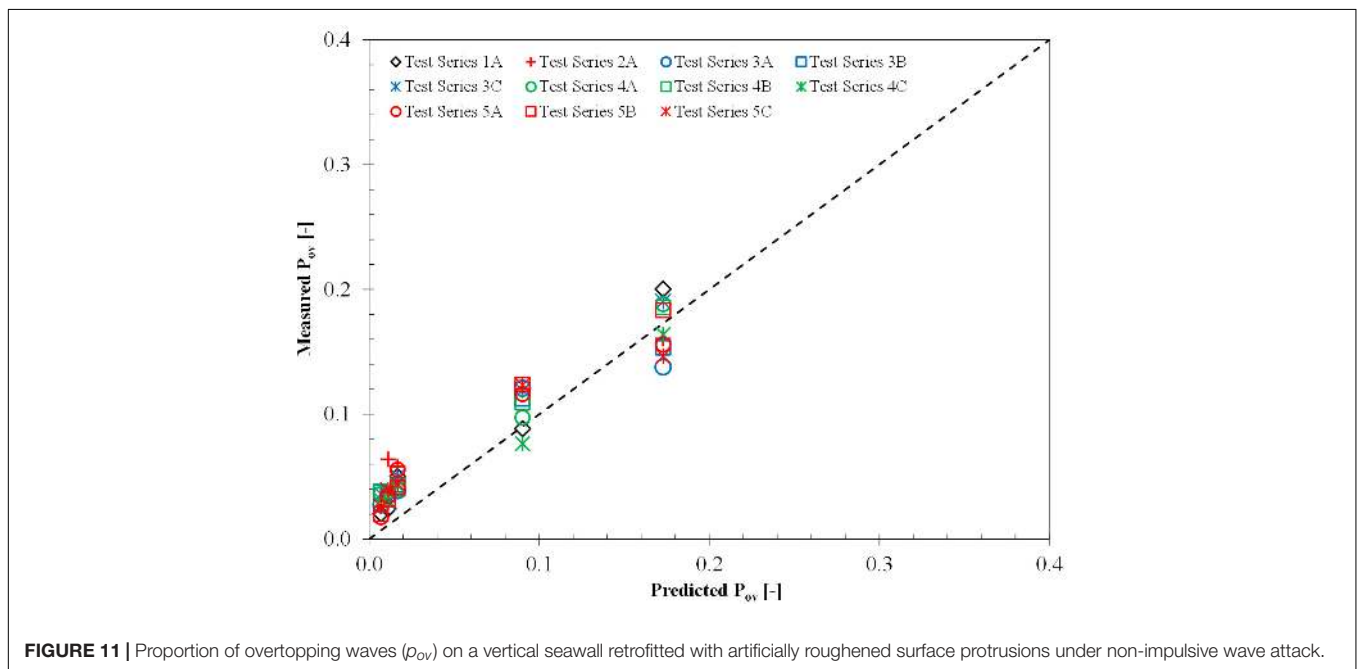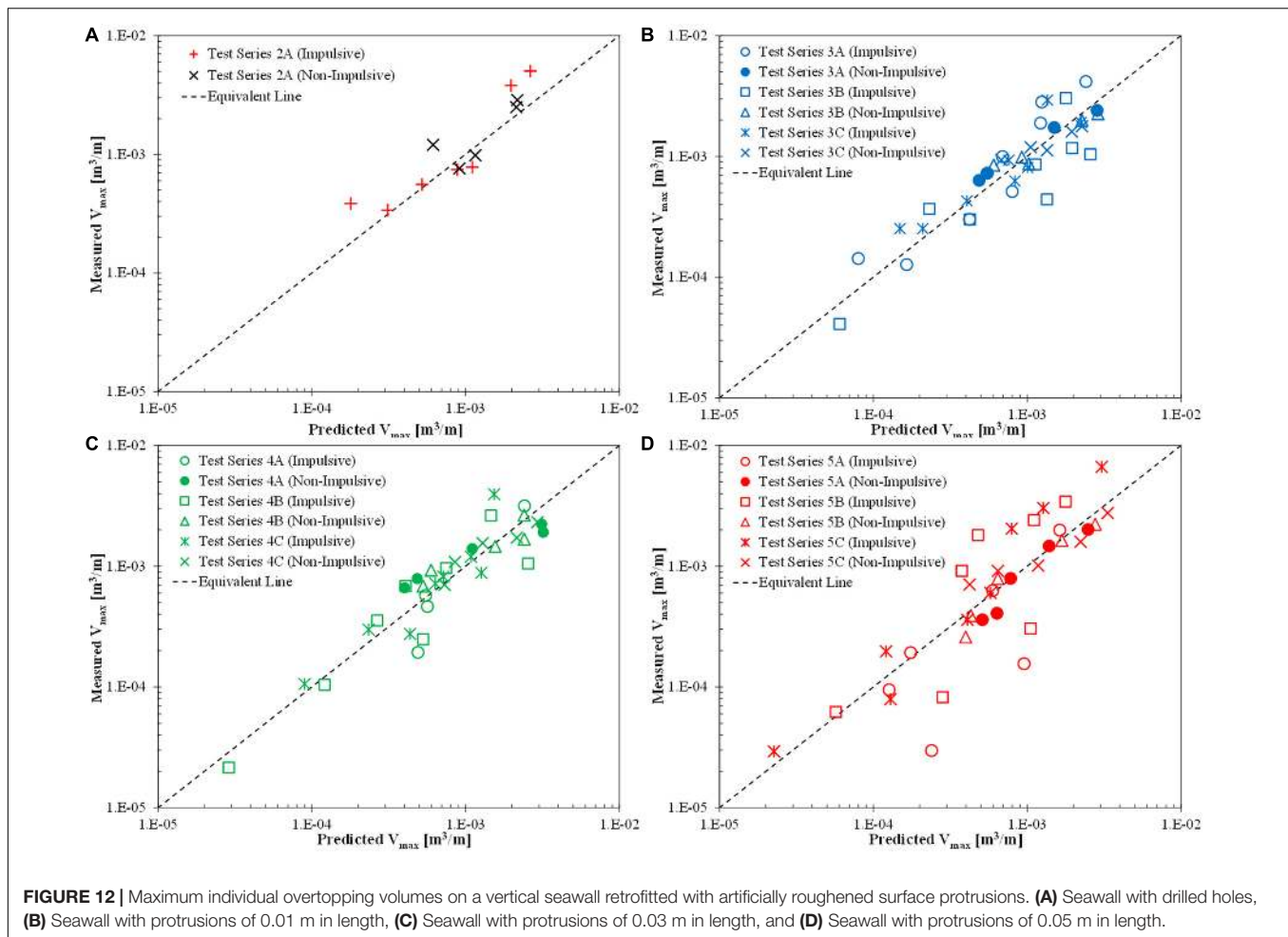

FIGURE 11 | Proportion of overtopping waves (p_{ov}) on a vertical seawall retrofitted with artificially roughened surface protrusions under non-impulsive wave attack.

reference condition as well as to the existing empirically-based predictions (**Figure 7A**).

For test configurations with surface protrusions, the data indicates that the mean overtopping rates are reduced for the cases of artificially roughened conditions when compared to empirical predictions from EurOtop II (**Figures 7B–D**). A comparison of results for Test Series 3A to 3C (**Figure 7B**), 4A to 4C (**Figure 7C**), and 5A to 5C (**Figure 7D**) indicate that reductions in mean overtopping rate increase with increasing density of surface elements. Similarly, comparing results for Series 3A to 5A, 3B to 5B, and 3C to 5C in **Figures 7B–D**

indicates that reductions in mean overtopping rate also increase with increasing length of surface elements. A consistent pattern regarding the dominance of either density or length in reducing overtopping rates does not emerge from the measured data, albeit results confirm that both density and length play a major role in reducing overtopping. As such, the greatest reduction in overtopping with respect to the reference condition (plain vertical wall) was observed for Series 5A in which the combined effect of both maximum density and length of roughness elements (98 stems/100 mm^2 and 0.05 m) were considered. Comparing results for Series 5A to those for the reference condition (Test Series

FIGURE 12 | Maximum individual overtopping volumes on a vertical seawall retrofitted with artificially roughened surface protrusions. **(A)** Seawall with drilled holes, **(B)** Seawall with protrusions of 0.01 m in length, **(C)** Seawall with protrusions of 0.03 m in length, and **(D)** Seawall with protrusions of 0.05 m in length.

1A) (**Figure 7D**) shows that reductions in overtopping rate are, on average, reduced by over 90% across the range of relative freeboards that were tested (1.58–3.33) but was at a maximum of c. 100% for the relative crest height of 2.86.

For non-impulsive wave conditions, the measured dimensionless mean overtopping discharge for all test cases with respect to the relative freeboard of the structure are shown in **Figure 8**. The empirical predictions of non-impulsive overtopping as predicted by EurOtop (2018) are also included in **Figure 8**. The results confirm that, for the wave conditions studied, the observed mean overtopping rates are consistent with the overall trend of empirical predictions proposed by EurOtop (2018), indicating that for the non-impulsive wave conditions, surface protrusions have a considerably lower impact on overtopping rates compared to impulsive wave conditions (**Figure 8**).

Probability of Overtopping Waves

The measured proportions of overtopping waves for the eco-retrofitting cases are compared with the empirical predictions of EurOtop (2018) in **Figure 9**. As expected, data for the vertical seawall containing the drilled recesses for the surface protrusions (Test Series 2A in **Figure 9A**) are entirely consistent

with predicted values of EurOtop (2018). More considerable departures from EurOtop predictions were however, observed for the test cases where the seawall roughening was more significant. **Figures 9B–D** shows the measured proportion of overtopping waves for the tests with surface protrusions of varying length scale and surface density. Comparing the results for Test Series 3A to 3C (**Figure 9B**), 4A to 4C (**Figure 9C**), and 5A to 5C (**Figure 9D**) and again for Series 3A to 5A, 3B to 5B, and 3C to 5C indicates that the proportion of overtopping waves reduces considerably as roughness (through increased density and/or increased length of surface protrusions) is added to the seawalls. As was the case with the mean overtopping rate, the maximum reduction in p_{ov} was observed for Test Series 5A where the proportion of overtopping waves across the range of tested relative freeboards was shown to be, on average, approximately 80% less than that predicted by EurOtop (2018), with no overtopping being observed for relative freeboards in excess of 2.86 (**Figure 10**).

The resulting proportion of overtopping waves for all experimental configurations that were tested under non-impulsive wave conditions, are compared with predictions from EurOtop (2018) in **Figure 11**. Results demonstrate that measured values of p_{ov} correlate reasonably well (within a factor of 2) with those predicted by EurOtop (2018), indicating that increases in

surface roughening for non-impulsive wave conditions have little effect on wave overtopping characteristics (**Figure 11**).

Maximum Individual Overtopping Volume

For the tests undertaken with artificially roughened seawalls, measured maximum individual overtopping volumes (V_{max}) are compared to EurOtop (2018) predictions in **Figure 12**. Measured data is shown to be in good agreement with empirical predictions. It is evident that for both impulsive and non-impulsive wave conditions, the surface protrusions have little impact on maximum wave-by-wave overtopping volumes. Data also indicate that surface protrusions contribute to a reduction in overtopping events (**Figure 9**), although V_{max} values remain comparable to those predicted from empirical formulations. The findings of this study for V_{max} are in-line with findings previously reported by Salauddin and Pearson (2019a) for vertical walls with shingle foreshores and by Salauddin and Pearson (2020) for sloping structures with permeable shingle slopes.

DISCUSSION AND CONCLUSION

The use of "hard" engineered coastal defence structures has, for the most part, remained the standard for the management of risks posed by sea and wave hazards, with seawalls and breakwaters featuring prominently in many flood alleviation schemes. A recent mapping exercise along the Ireland and Wales Irish Sea coastline for example, identified 6,886 artificial structures, the density of which was significantly higher in urbanised areas (reaching up to 28 structures per km of coastline) where the risks to human assets would be most acute. Of the structures that were characterised and quantified in this study, 32% were seawalls (Thompson et al., in review). Notwithstanding the body of evidence that highlights differences in the abundance and species richness of benthic organisms supported by artificial structures compared to natural systems (Chapman, 2003), the implementation of "hard" structures has, until recently, remained largely unchallenged. This situation, however, is now increasingly being questioned with researchers (see for example, Browne and Chapman, 2011; Chapman and Underwood, 2011; Firth et al., 2013, 2016; Temmerman et al., 2013; Bouma et al., 2014; Browne and Chapman, 2014; Evans et al., 2016; Morris et al., 2017, 2018; Strain et al., 2018a; O'Shaughnessy et al., 2020) highlighting the potential of "eco-engineering" or "hard eco-engineering" coastal defence solutions to fulfil the requirements of conventional "hard" sea defence structures while at the same time addressing the deficits in benthic biodiversity and ecosystem functioning that arise from these "hard" defences. Studies, however, assessing "eco-engineering" interventions, and specifically those that directly compare performance levels to "hard" engineered structures under comparable environmental conditions, remain limited. The likelihood therefore of "hard" structures continuing to feature prominently in coastal protection schemes, coupled with the prevalence of existing artificial structures in our marine settings, has driven a parallel research effort that has focused on ways of mitigating the negative ecological impacts associated with "hard" structures. In this regard, "additive" measures such as the introduction to seawalls of artificial water filled depressions (e.g., vertipools, bolt on rock pools, and flowerpots) and textured tiles as well as "subtractive" interventions such as adding holes to an existing structures have gained traction within the scientific community where richness in biodiversity of fish and benthic organisms has shown to be positively correlated to the topographical complexity of marine infrastructure (Chapman and Underwood, 2011; Browne and Chapman, 2014; Firth et al., 2014a,b; Perkol-Finkel and Sella, 2015; Evans et al., 2016; Hall et al., 2018, 2019).

An aspect of these "additive" measures that has received comparatively little attention is whether they offer a dual benefit of also serving to dissipate wave energy and reduce overtopping and its associated hazard. Contributing to this research question served as the motivation for the present study, in which the overtopping performance of artificially roughened vertical seawalls was evaluated under controlled laboratory conditions, with different configurations of surface protrusions being tested for both impulsive and non-impulsive wave conditions. It was found that the increased roughening from surface protrusions (increasing the length and/or density) plays a pivotal role in reducing the dimensionless mean overtopping rates on the seawall. Reductions in dimensionless mean overtopping rate (by up to 100% in comparison to the plain seawall reference condition) were confined to impulsive (violent) wave conditions, with no significant differences (for all tested roughness configurations) in mean overtopping rates being observed for non-impulsive wave conditions compared to the plain vertical seawall (reference condition). Given that the wave impact hazards on sea defences and in surrounding areas are significantly higher for impulsive wave attacks, the finding of reduced overtopping for impulsive or violent wave conditions is arguably more relevant for engineers and regulatory agencies charged with the design and construction of marine infrastructure. Measured overtopping rates for non-impulsive wave conditions that were tested were shown therefore to be consistent with empirical (EurOtop II) predictions. The greatest reductions in wave overtopping for the impulsive wave conditions were, unsurprisingly, observed for the test case where both the density and length of protrusion was at its highest. The proportion of waves that overtopped the seawalls was also shown to reduce significantly (by up to 100%) as the roughness of the seawall was increased, the maximum reduction again being observed for the test case where both the length and density of protrusion was at its highest. While scaled models of eco-interventions were not in themselves tested, experiments where the roughness characteristics of vertical seawalls were increased, allowed for the effects of increased surface complexity (akin to many "additive" eco-engineering interventions) on overtopping of sea defence structures to be considered. The results suggest that the addition of eco-engineering interventions to existing seawalls can serve a dual role in that (in addition to ecological enhancement) wave heights and wave energy can be decreased, mitigating wave overtopping and reducing flood risks behind sea defences. Given

the ongoing need to enhance the resilience of existing sea defence structures in the face of the increasing frequency and severity of extreme climatic events, the results of this study are significant. For the first time, the potential for specific arrays of "additive" ecological measures on sea defence structures to mitigate wave-overtopping of impulsive waves has been highlighted.

In addition to additive features, subtractive features of drilled holes on seawalls were also tested in this study. The capacity of these "subtractive" interventions in reducing overtopping was not proven, but likewise, they were not shown on have a negative effect on the overtopping characteristics of the seawall and therefore do not compromise the engineering outcomes of the structure.

Notwithstanding the results of this and previous studies, it is likely that the wide adoption of eco-engineering interventions for habitat enhancement and/or mitigation of wave overtopping hazard will continue to face challenges and satisfactorily addressing concerns of regulatory agencies regarding the longer-term maintenance and sustainability implications arising from "artificially" modifying sea defence structures will need to be addressed. Furthermore, engineering design guidance for predicting wave overtopping characteristics, exists only for plain vertical walls. In the absence of specific guidance relating to ecologically modified seawalls, we recommend a conservative prediction of maximum individual overtopping volumes at vertical seawalls with solid foreshore slopes i.e., the predictions as stated by EurOtop (2018).

A challenge in the small-scale physical modelling of wave environments is understanding and quantifying the effects of scale on experimental results. It has been shown previously that scale and model effects in studies of wave overtopping on vertical or near-vertical impermeable seawalls undertaken in small-scale wave flumes (of the scale used in this study) are minimal [see for example, study of wave overtopping on vertical seawalls by Pearson et al. (2002), the findings of which were later incorporated into EurOtop (2018)]. The test set-up in the current study also followed accepted wave flume investigation guidelines (Wolters et al., 2009; EurOtop, 2018) and given that measurements of incident wave heights followed the conventional Rayleigh distribution and that overtopping characteristics were consistent with empirical predictions, the authors are satisfied that scale and model effects in designing wave conditions were not significant. However, given the paucity of data at prototype scale pertaining to the addition of surface

roughness of the type tested, scale effects in this regard could not be quantified. Further validation of test measurements with surface elements at both small and larger scales is clearly desirable to explore any potential scaling effects from these elements under laboratory and prototype conditions. Notwithstanding these limitations, the study contributes to our understanding of the effects on wave overtopping from increasing the topographic complexity of sea defence structures for impulsive and non-impulsive wave conditions.

DATA AVAILABILITY STATEMENT

The raw data supporting the conclusions of this article will be made available by the authors, without undue reservation.

AUTHOR CONTRIBUTIONS

MS, JO'S, SA, and JP conceived, designed the study, and developed the manuscript draft. MS performed the laboratory experiments, generated the data, and conducted the data analysis. All authors contributed to the review in the manuscript and approved the final manuscript.

FUNDING

ACKNOWLEDGMENTS

SUPPLEMENTARY MATERIAL

The Supplementary Material for this article can be found online at: https://www.frontiersin.org/articles/10.3389/fmars.2021.674630/full#supplementary-material

REFERENCES

Abolfathi, S., Dong, S., Borzooei, S., Yeganeh-Bakhtiari, A., and Pearson, J. (2018). "Application of smoothed particle hydrodynamics in evaluating the performance of coastal retrofits structures," in *Proceedings.of the 36th Conference on Coastal Engineering*, (Baltimore MD), doi: 10.9753/icce.v36.papers.109

Allsop, N. W. H., Bruce, T., Pearson, J., and Besley, P. (2005). "Wave overtopping at vertical and steep seawalls," in *Proceedings of the International Conference on Maritime Engineering, Institution of Civil Engineers, 158(MA3)* (UK), 103–114. doi: 10.1680/maen.2005.158.3.103

Allsop, N. W. H., Vicinanza, D., and Mckenna, J. (1996). *Wave Forces on Vertical and Composite Breakwaters. Research Report SR 443*. Wallingford: HR Wallingford.

Barbier, E. B., Hacker, S. D., Kennedy, C., Koch, E. W., Stier, A. C., and Silliman, B. R. (2011). The value of estuarine and coastal ecosystem services. *Ecol. Monogr.* 81, 169–193.

Battjes, J. A., and Groenendijk, H. W. (2000). Wave height distributions on shallow foreshores. *Coast. Eng.* 40, 161–182. doi: 10.1016/s0378-3839(00)00007-7

Besley, P. (1998). *Overtopping of Seawalls – Design and Assessment Manual. R&D Technical Report W 178*. Bristol: Environment Agency. .

Birkeland, J. (2003). "Beyond zero waste. societies for a sustainable future," in *Proceedings of the 3rd UKM-UC International Conference 14-15 April*, (Canberra).

Birkeland, J. (2009). "Eco-retrofitting with building integrated living systems," in *Proceedings of the 3rd CIB International Conference on Smart and Sustainable Built Environment*, ed. A. van den Dobbelsteen (Netherlands: Delft University of Technology), 1–9.

Borsje, B. W., Van Wesenbeeck, B. K., Dekker, F., Paalvast, P., Bouma, T. J., Van Katwijk, M. M., et al. (2011). How ecological engineering can serve in coastal protection. *Ecol. Eng.* 37, 113–122. doi: 10.1016/j.ecoleng.2010.11.027

Bouma, T. J., Van Belzen, J., Balke, T., Zhu, Z., Airoldi, L., Blight, A. J., et al. (2014). Identifying knowledge gaps hampering application of intertidal habitats in coastal protection: Opportunities & steps to take. *Coastal Eng.* 87, 147–157. doi: 10.1016/j.coastaleng.2013.11.014

Browne, M. A., and Chapman, M. G. (2011). Ecologically informed engineering reduces loss of intertidal biodiversity on artificial shorelines. *Environ. Sci. Technol.* 45, 8204–8207. doi: 10.1021/es201924b

Browne, M. A., and Chapman, M. G. (2014). Mitigating against the loss of species by adding artificial intertidal pools to existing seawalls. *Mar. Ecol. Prog. Ser.* 497, 119–129. doi: 10.3354/meps10596

Bruce, T., Van der Meer, J. W., Franco, L., and Pearson, J. M. (2009). vertopping performance of different armour units for rubble mound breakwaters. *Coastal Eng.* 56, 166–179. doi: 10.1016/j.coastaleng.2008.03.015

Bruce, T., Van Der Meer, J. W., Pullen, T., and Allsop, N. W. H. (2010). "Wave overtopping at vertical and steep structures," in *Chapter 16 in Handbook of Coastal and Ocean Engineering*, ed. Y. C. Kim (Singapore: World Scientific).

Chapman, M. G. (2003). Paucity of mobile species on constructed seawalls: effects of urbanization on biodiversity. *Mar. Ecol. Prog. Ser.* 264, 21–29. doi: 10.3354/meps264021

Chapman, M. G., and Underwood, A. J. (2011). Evaluation of ecological engineering of "armoured" shorelines to improve their value as habitat. *J. Exp. Mar. Biol. Ecol.* 400, 302–313. doi: 10.1016/j.jembe.2011.02.025

Dafforn, K. A., Glasby, T. M., Airoldi, L., Rivero, N. K., Mayer-Pinto, M., and Johnston, E. L. (2015). Marine urbanization: an ecological framework for designing multifunctional artificial structures. *Front. Ecol. Environ.* 13:82–90. doi: 10.1890/140050

Dong, S., Abolfathi, S., Salauddin, M., and Pearson, J. M. (2020a). Spatial distribution of wave-by-wave overtopping at vertical seawalls. *Coastal Eng. Proc.* 36:17. doi: 10.9753/icce.v36v.structures.17

Dong, S., Abolfathi, S., Salauddin, M., Tan, Z. H., and Pearson, J. M. (2020b). Enhancing climate resilience of vertical seawall with retrofitting - a physical modelling study. *Appl. Ocean Res.* 103:102331. doi: 10.1016/j.apor.2020.102331

Dong, S., Salauddin, M., Abolfathi, S., Tan, Z. H., and Pearson, J. M. (2018). The influence of geometrical shape changes on wave overtopping: a laboratory and sph numerical study. *Coasts Mar. Struct. Breakwaters* 2017, 1217–1226. doi: 10.1680/cmsb.63174.1217

EurOtop (2018). *Manual on Wave Overtopping of Sea Defences and Related Structures*, 2nd Edn. Available online at: www.overtopping-manual.com (accessed February 2, 2021).

Evans, A. J., Firth, L. B., Hawkins, S. J., Hall, A. E., Ironside, J. E., Thompson, R. C., et al. (2019). From ocean sprawl to blue-green infrastructure–A UK perspective on an issue of global significance. *Environ. Sci. Policy* 9, 60–69. doi: 10.1016/j.envsci.2018.09.008

Evans, A. J., Firth, L. B., Hawkins, S. J., Morris, E. S., Goudge, H., and Moore, P. J. (2016). Drill-cored rock pools: an effective method of ecological enhancement on artificial structures. *Mar. Freshwater Res.* 67, 123–130. doi: 10.1071/MF14244

Evans, A. J., Lawrence, P. J., Natanzi, A. S., Moore, P. J., Davies, A. J., Crowe, T. P., et al. (2021). Replicating natural topography on marine artificial structures–A novel approach to eco-engineering. *Ecol. Eng.* 160:106144. doi: 10.1016/j.ecoleng.2020.106144

Firth, L. B., Browne, K. A., Knights, A. M., Hawkins, S. J., and Nash, R. (2016). Eco-engineered rock pools: a concrete solution to biodiversity loss and urban sprawl in the marine environment. *Environ. Res. Lett.* 11:094015. doi: 10.1088/1748-9326/11/9/094015

Firth, L. B., Schofield, M., White, F. J., Skov, M. W., and Hawkins, S. J. (2014a). Biodiversity in intertidal rock pools: Informing engineering criteria for artificial habitat enhancement in the built environment. *Mar. Environ. Res.* 102, 122–130. doi: 10.1016/j.marenvres.2014.03.016

Firth, L. B., Thompson, R. C., Bohn, K., Abbiati, M., Airoldi, L., Bouma, T. J., et al. (2014b). Between a rock and a hard place: environmental and engineering considerations when designing coastal defence structures. *Coastal Eng.* 87, 122–135. doi: 10.1016/j.coastaleng.2013.10.015

Firth, L. B., Thompson, R. C., White, F. J., Schofield, M., Skov, M. W., Hoggart, S. P. G., et al. (2013). The importance of water-retaining features for biodiversity

on artificial intertidal coastal defence structures. *Divers. Distrib.* 19, 1275–1283. doi: 10.1111/ddi.12079

Franco, L., De Gerloni, M., and Van Der Meer, J. W. (1994). "Wave overtopping on vertical and composite breakwaters," in *Proceedings of the 24th ICCE, ASCE, Kobe*, (Japan), 1030–1045.

Goda, Y. (2009). Derivation of unified wave overtopping formulas for seawalls with smooth, impermeable surfaces based on selected CLASH datasets. *Coastal Eng.* 56, 385–399. doi: 10.1016/j.coastaleng.2008.09.007

Hall, A. E., Herbert, R. J. H., Britton, J. R., and Hull, S. L. (2018). Ecological enhancement techniques to improve habitat heterogeneity on coastal defence structures. *Estuarine Coastal Shelf Sci.* 210, 68–78. doi: 10.1016/j.ecss.2018.05.025

Hall, A. E., Herbert, R. J. H., Britton, R. J., Boyd, I., and George, N. (2019). Shelving the coast with vertipools: retrofitting artificial rock pools on coastal structures as mitigation for coastal squeeze. *Front. Mar. Sci.* 6:456.

IPCC (2014). *Climate Change 2014: Synthesis Report. Contribution of Working Groups I, II and III to the Fifth Assessment Report of the Intergovernmental Panel on Climate Change.* Geneva: IPCC.

IPCC (2018). *Global Warming of 1.5°C: An IPCC Special Report on the Impacts of Global Warming of 1.5° C Above Pre-industrial Levels and Related Global Greenhouse Gas Emission Pathways, in the Context of Strengthening the Global Response to the Threat of Climate Change, Sustainable Development, and Efforts to Eradicate Poverty, Intergovernmental Panel on Climate Change.* Geneva: IPCC.

MacArthur, M., Naylor, L. A., Hansom, J. D., Burrows, M. T., and Boyd, I. (2018). *Ecological Enhancement of Coastal Infrastructure Coasts, Marine Structures and Breakwaters 2017: Realising the Potential.* London: ICE Publishing, 279–282.

Mansard, E. P. D., and Funke, E. R. (1980). "The measurement of incident and reflected spectra using a least squares method," in *Proceedings of the Conf. on Coastal Engineering (ICCE), 1980*, (Sydney), 154–172.

Morris, R. L., Chapman, M. G., Firth, L. B., and Coleman, R. A. (2017). Increasing habitat complexity on seawalls: Investigating large-and small-scale effects on fish assemblages. *Ecol. Evol.* 7, 9567–9579. doi: 10.1002/ece3.3475

Morris, R. L., Konlechner, T. M., Ghisalberti, M., and Swearer, S. E. (2018). From grey to green: Efficacy of eco-engineering solutions for nature-based coastal defence. *Glob. Chang. Biol.* 24, 1827–1842. doi: 10.1111/gcb.14063

Naylor, L. A., Coombes, M. A., Kippen, H., Horton, B., Gardiner, T., Cordell, M. R., et al. (2018). "Developing a business case for greening hard coastal and estuarine infrastructure: preliminary results," in *Proceedings of the Coasts, Marine Structures and Breakwaters 2017*, (London: Institution of Civil Engineers).

Naylor, L. A., Kippen, H., Coombes, M. A., Horton, B., Macarthur, M., and Jackson, N. (2017). *Greening the Grey: a Framework for Integrated Green grey Infrastructure (IGGI).* Glasgow: University of Glasgow.

O'Shaughnessy, K. A., Hawkins, S. J., Evans, A. J., Hanley, M. E., Lunt, P., Thompson, R. C., et al. (2020). Design catalogue for eco-engineering of coastal artificial structures: a multifunctional approach for stakeholders and end-users. *Urban Ecosystems* 23, 431–443. doi: 10.1007/s11252-019-00924-z

O'Sullivan, J. J., Salauddin, M., Abolfathi, S., and Pearson, J. M. (2020). Effectiveness of eco-retrofits in reducing wave overtopping on seawalls. *Coastal Eng. Proc.* 36:13. doi: 10.9753/icce.v36v.structures.13

Oumeraci, H. (1994). Review and analysis of vertical breakwater failures - lessons learned. *Coastal Eng.* 22, 3–29. doi: 10.1016/0378-3839(94)90046-9

Pearson, J. M., Bruce, T., and Allsop, N. W. H. (2001). "Prediction of wave overtopping at steep seawalls—variabilities and uncertainties," in *Proceedings of the Conference on Waves '01, ASCE*, (San Francisco CA), 1797–1808.

Pearson, J. M., Bruce, T., Allsop, N. W. H., and Gironella, X. (2002). "Violent wave overtopping-measurements at large and small scale," in *Proceedings of the 28th International Coastal Engineering Conference, ASCE*, (Cardiff), 2227–2238.

Perkol-Finkel, S., and Sella, I. (2015). "Harnessing urban coastal infrastructure for ecological enhancement," in *Proceedings of the Institution of Civil Engineers-Maritime Engineering, 2015*, Vol. 168, (London: Thomas Telford Ltd), 102–110. doi: 10.1680/jmaen.15.00017

Pontee, N., Narayan, S., Beck, M. W., and Hosking, A. H. (2016). "Nature-based solutions: lessons from around the world," in *Proceedings of the Institution of*

Civil Engineers-Maritime Engineering Conference, (London: Thomas Telford Ltd), 29–36.

Pullen, T., Allsop, N. W. H., Bruce, T., Kortenhaus, A., Schüttrumpf, H., and Van der Meer, J. W. (2007). *EurOtop Wave Overtopping of Sea Defences and Related Structures: Assessment Manual*. Heide: Boyens Medien GmbH.

Salauddin, M., Broere, A., Van der Meer, J. W., Verhagen, H. J., and Bijl, E. (2017). First tests on the symmetrical breakwater armor unit crablock. *Coastal Eng. J.* 59, 1–33. doi: 10.1142/S0578563417500206

Salauddin, M., O'Sullivan, J. J., Abolfathi, S., and Pearson, J. M. (2020a). "Extreme wave overtopping at ecologically modified sea defences," in *Proceedings of the EGU General Assembly 2020, Online, 4–8 May 2020, EGU2020-6162* (Online), doi: 10.5194/egusphere-egu2020-6162

Salauddin, M., O'Sullivan, J. J., Abolfathi, S., Dong, S., and Pearson, J. M. (2020b). Distribution of individual wave overtopping volumes on a sloping structure with a permeable foreshore. *Coastal Eng. Proc.* 36:54. doi: 10.9753/icce.v36v.papers.54

Salauddin, M., and Pearson, J. M. (2018). A laboratory study on wave overtopping at vertical seawalls with a shingle foreshore. *Coastal Eng. Proc.* 1:waves.56. doi: 10.9753/icce.v36.waves.56

Salauddin, M., and Pearson, J. M. (2019a). Wave overtopping and toe scouring at a plain vertical seawall with shingle foreshore: a Physical model study. *Ocean Eng.* 171, 286–299. doi: 10.1016/j.oceaneng.2018.11.011

Salauddin, M., and Pearson, J. M. (2019b). Experimental study on toe scouring at sloping walls with gravel foreshores. *J. Mar. Sci. Eng.* 7:198. doi: 10.3390/jmse7070198

Salauddin, M., and Pearson, J. M. (2020). Laboratory investigation of overtopping at a sloping structure with permeable shingle foreshore. *Ocean Eng.* 197, 1–13. doi: 10.1016/j.oceaneng.2019.106866

Strain, E., Morris, R., and Bishop, M. (2017). *Sydney Harbour: Enhancing Seawall Sustainability*. Canberra, AUS: NSW Department of Primary Industries.

Strain, E. M. A., Morris, R. L., Coleman, R. A., Figueira, W. F., Steinberg, P. D., Johnston, E. L., et al. (2018a). Increasing microhabitat complexity on seawalls can reduce fish predation on native oysters. *Ecol. Eng.* 120, 637–644. doi: 10.1016/j.ecoleng.2017.05.030

Strain, E. M. A., Olabarria, C., Mayer-Pinto, M., Cumbo, V., Morris, R. L., Bugnot, A. B., et al. (2018b). Eco-engineering urban infrastructure for marine and coastal biodiversity: which interventions have the greatest ecological benefit? *J. Appl. Ecol.* 55, 426–441. doi: 10.1111/1365-2664.12961

TAW (2002). "Technical report wave run-up and wave overtopping at dikes," in *TAW Report (Incorporated in the EurOtop manual)*, ed. J. W. Van der Meer, Delft: Rijkswaterstaat.

Temmerman, S., Meire, P., Bouma, T. J., Herman, P. M., Ysebaert, T., and De Vriend, H. J. (2013). Ecosystem-based coastal defence in the face of global change. *Nature* 504, 79–83. doi: 10.1038/nature12859

Van der Meer, J. W., and Janssen, J. P. F. M. (1994). "Wave run-up and wave overtopping at dikes," in *Wave forces on Inclined and Vertical Wall Structures*, eds N. Kobayashi and Z. Demirbilek (RestonVA: ASCE), 1–27.

Victor, L., Van der Meer, J. W., and Troch, P. (2012). Probability distribution of individual wave overtopping volumes for smooth impermeable steep slopes with low crest freeboards. *Coastal Eng.* 64, 87–101. doi: 10.1016/j.coastaleng.2012.01.003

Vitousek, S., Barnard, P. L., Fletcher, C. H., Frazer, N., Erikson, L., and Storlazzi, C. D. (2017). Doubling of coastal flooding frequency within decades due to sea-level rise. *Sci. Rep.* 7, 1–9.

Vuik, V., Jonkman, S. N., Borsje, B. W., and Suzuki, T. (2016). Nature-based flood protection: the efficiency of vegetated foreshores for reducing wave loads on coastal dikes. *Coastal Eng.* 116, 42–56. doi: 10.1016/j.coastaleng.2016.06.001

Waltham, N. J., and Sheaves, M. (2020). Thermal exposure risks to mobile tropical marine snails: are eco-engineered rock pools on seawalls scale-specific enough for comprehensive biodiversity outcomes? *Mar. Pollut. Bull.* 156:111237. doi: 10.1016/j.marpolbul.2020.111237

Wolters, G., Van Gent, M., Allsop, N. W. H., Hamm, L., and Mühlestein, D. (2009). "HYDRALAB III: guidelines for physical model testing of rubble mound breakwaters," in *Proceedings of the 9th International Conference on Coasts, Marine Structures and Breakwaters: Adapting to Change*, (Edinburgh), 659–670.

Zanuttigh, B., Van Der Meer, J. W., Bruce, T., and Hughes, S. (2013). "Statistical characterisation of extreme overtopping wave volumes," in *Proceedings of the ICE, Coasts, Marine Structures and Breakwaters*, (Edinburgh).

NOTATIONS

Symbol	Meaning	Unit
a	Scale parameter in Weibull distribution	[−]
b	Shape parameter in Weibull distribution	[−]
g	Gravitational acceleration	[m/s^2]
h_t	Water depth at toe of the structure	[m]
H	Individual wave height	[m]
H_m	Mean wave height	[m]
H_{m0}	Significant wave height determined from spectra analysis	[m]
I_r	Iribarren number or breaker parameter	[−]
$L_{m-1,0}$	Spectral wave length based on linear theory ($gT_{m-1,0}^2/2\pi$)	[m]
N_{ow}	Number of overtopping waves	[−]
N_w	Number of incident waves	[−]
P_{ow}	Probability of overtopping per wave (N_{ow}/N_w)	[−]
$P(V)$	Probability of exceedance of overtopping volume	[−]
q	Mean overtopping discharge per m width	[m^3/s per m]
R_c	Crest freeboard	[m]
s_m	Wave steepness based on average wave period ($2\pi H_{m0}/gT_m^2$)	[−]
$s_{m-1,0}$	Wave steepness based on mean spectral period ($2\pi H_{m0}/gT_{m-1,0}^2$)	[−]
s_{op}	Wave steepness for spectral peak period ($2\pi H_{m0}/gT_p^2$)	[−]
T_m	Average wave period calculated from time series analysis	[s]
$T_{m-1,0}$	Average spectral wave period defined from spectral analysis by m_{-1}/m_0	[s]
T_p	Spectral peak wave period	[s]
V	Volume of overtopping wave per m width	[m^3 per m]
V_{bar}	Mean overtopping volume per m width	[m^3 per m]
V_{max}	Maximum individual overtopping volume per m width	[m^3 per m]
α	Slope of the structure	[radians]
γ	Peak enhancement factor of JONSWAP energy spectrum	[−]
Γ	Mathematical gamma function	[−]